

# Reducing neutral point voltage fluctuation in NPC three-level active power filters

Peng Qian<sup>1\*</sup> Xiandong Ma<sup>1</sup> Guohai Liu<sup>2</sup> Zhaoling Chen<sup>2</sup>

<sup>1</sup> Engineering Department, Lancaster University, Lancaster LA1 4YW, United Kingdom; p.qian@lancaster.ac.uk, xiandong.ma@lancaster.ac.uk

<sup>2</sup> College of Electrical and Information Engineering, Jiangsu University, Zhenjiang, China; ghliu@ujs.edu.cn, czl908@126.com

\* Correspondence: p.qian@lancaster.ac.uk; Tel: +44 (0)1524 593700

**Abstract:** Shunt active power filters (SAPFs) have been widely used to improve power quality of the grid by mitigating harmonics injected from nonlinear loads. This paper presents a new method for improving the performance of SAPFs using neutral point clamped (NPC) three-level inverters. NPC three-level inverters often suffer excessive voltage fluctuations at the neutral-point of DC-link capacitors, which may damage switching devices and cause additional high harmonic distortion of the output voltage. In order to solve the problem, two compensating schemes are proposed to restrict voltage fluctuation in the inverters. The first is voltage dependent, adopting a voltage compensation method, while the second is current dependent, using a current compensation method. The paper describes the respective circuit architectures and principles of operation. Corresponding models are mathematically formulated and evaluated under typical balanced and unbalanced working load conditions. The results show that both schemes are able to alleviate considerably voltage oscillations and hence harmonic distortions, and the current compensated NPC inverter outperforms the voltage compensated NPC inverter. Consequently, it is shown that the proposed approaches are effective and feasible for improving power quality of the grid when connected to nonlinear loads.

**Keywords:** shunt active power filter (SAPF), three-level inverter, neutral point clamped (NPC), DC-link, voltage compensation, current compensation

---

## Symbols and abbreviations

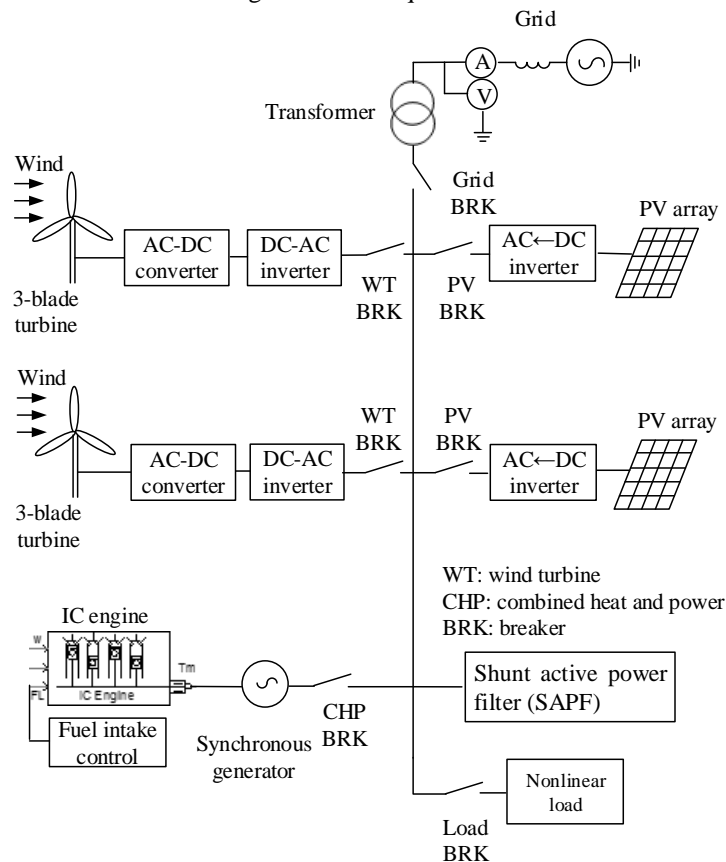
|                                 |   |
|---------------------------------|---|
| SAPF                            | Shunt active power filters                                  |
| NPC                             | Neutral point clamped                                       |
| DG                              | Distributed generation                                      |
| PV                              | Photovoltaics   |
| THD                             | Total harmonic distortion                                   |
| SVPWM                           | Space voltage vector pulse-width modulation                 |
| VNPC1                           | Voltage dependent NPC three-level inverter                  |
| CNPC1                           | Current controlled NPC three-level inverter                 |
| IGBT                            | Insulated gate bipolar transistor                           |
| $u_{sa}, u_{sb}, u_{sc}$        | Three-phase alternating-current supply                      |
| $i_{sa}, i_{sb}, i_{sc}$        | Grid currents   |
| $i_{La}, i_{Lb}, i_{Lc}$        | Load currents   |
| $i_{ca}, i_{cb}, i_{cc}$        | Compensation currents provided by the SAPF                  |
| $u_o$                           | Neutral point voltage of the three-phase bridge arm         |
| $u_N$                           | Neutral point voltage of the DC-link capacitors             |
| $u_c$                           | Voltage of the primary side of the transformer              |
| $u_b$                           | Compensating voltage  |
| $u_s$                           | DC-link voltage applied across the capacitors               |
| $S_1, S_2, S_3, S_4$            | IGBT power switches   |
| T                               | Coupling transformer  |
| L, C <sub>f</sub>               | LC filter   |
| $u_{dc}$                        | DC voltage applied to the single-phase full-bridge inverter |
| $u_i$                           | Voltage output of the single-phase inverter                 |
| $i_1$                           | Current through the filter inductor                         |
| $i_2$                           | Transformer primary side current                            |
| $i_{cf}$                        | Current through the filter capacitor                        |
| D <sub>1</sub>                  | Diode used to prevent reverse current flow                  |
| L <sub>2</sub> , C <sub>3</sub> | LC filter   |
| $u_{dc1}$                       | Voltage input of the boost DC/DC converter                  |
| $u_{dc2}$                       | Voltage output of the boost DC/DC converter                 |

|    |               |   |
|----|---------------|---|
| 56 | $i_{c3(off)}$ | Current in capacitor $C_3$ when switching device $S_5$ is turned off        |
| 57 | $i_3$         | Current in the inductor $L_1$   |
| 58 | $i_4$         | Compensating current  |
| 59 | $u_{LI(off)}$ | Voltage across the inductor $L_1$ when switching device $S_5$ is turned off |
| 60 | $u_{LI(on)}$  | Voltage across inductor $L_1$ when switch $S_5$ is turned on                |
| 61 | $D$           | Duty cycle of the switching device $S_5$                                    |
| 62 | $K_p, K_i$    | Parameters of the PI controller   |

63

64 **1. Introduction**

65 Recently, distributed generation (DG) installation has been significantly increased, due to the deregulation  
66 of utilities, environmental constraints, and concerns regarding climate change [1]. This type of power generation  
67 system, as shown in Fig. 1, can provide electric power at or on a site closer to end users. However, harmonic-  
68 related problems have become a key concern because DG generators, such as wind and photovoltaics (PV), are  
69 coupled to power electronic converters and nonlinear loads [2]. In this regard, shunt active power filters (SAPFs)  
70 are widely used to mitigate these harmonic distortion problems in the grid. Compared to traditional two-level  
71 voltage-source inverters used in SAPFs, three-level voltage-source inverters are able to bear higher voltage  
72 classes and operate with lower harmonic distortion and at lower switching frequencies. Three-level inverters  
73 therefore offer better performance, in particular for medium-voltage applications [3]. In terms of topological  
74 structure, three-level inverters can be classified as one of three distinct types, namely diode clamped multilevel  
75 inverters, clamping capacitor multilevel inverters, and isolated H-bridge multilevel inverters [4-5]. The neutral  
76 point clamped (NPC) three-level inverter [6] is classified as type of diode clamped multilevel inverters. The  
77 most commonly used NPC three-level inverter circuit [7-9] is shown in Fig. 2, where it is incorporated into a  
78 SAPF. A full description of the circuit will be given in subsequent sections.



79 **Figure 1.** Schematic diagram of a distributed generation system

80

81

82

83

84

In a NPC three-level inverter, the neutral point of the DC-link capacitors and the neutral point of the three-phase bridge circuit are linked together directly. The neutral-point voltage of the three-phase bridge arm will vary because of the oscillation of the neutral-point voltage in the DC-link. The problem is inherent because

85 there is a neutral-point current flowing into or out of the neutral points in the circuit [10-11]. The varying current  
86 causes a charge-discharge phenomenon associated with the capacitors through the neutral-points in the circuit,  
87 thus resulting in a fluctuation in the neutral-point voltage. Consequently, the voltage ripples produced will affect  
88 the capability of the NPC three-level inverter to work efficiently [12]. Furthermore, excessive fluctuations of  
89 the DC-link voltage increase voltage stresses on the switching devices and hence the total harmonic distortion  
90 (THD) of the output current, which may limit potential engineering applications of this type of inverter.

91 There are three main factors that may cause oscillations in the neutral-point voltage in the DC-link branch.  
92 Firstly, the capacitance associated with the DC-link capacitors may become unbalanced after use for extended  
93 periods of time. DC link capacitors are required to endure high ripple currents leading to self-heating, which,  
94 in addition to high ambient operating temperatures, can result in the deterioration of the electrolyte material and  
95 the loss of electrolyte by vapour diffusion. Secondly, a critical factor for the inverter to work is delivery of the  
96 gate drive signals to the switching devices, as controlled by the switching frequency. Any switching delay will  
97 cause load current imbalance. Thirdly, nonlinear loads also cause harmonics to appear in the load current, which  
98 may in turn inject harmonics back to the inverter. Mathematical descriptions regarding the causes of voltage  
99 oscillations can be found in [13].

100 In order to solve these problems, three main methods have been investigated to alleviate voltage  
101 oscillations. The first is through the use of two independent DC sources to ensure a stable and constant DC  
102 voltage across the inverter. The method is expensive [14], because two independent DC sources require two  
103 isolation transformers. The second involves the design of improved control strategies, which are arguably the  
104 most widely used techniques at present [15-17]. Among the control strategies, the best known is the space  
105 voltage vector pulse-width modulation (SVPWM) method [18-22]. The control strategy proposed in [18]  
106 replaces the P-type or N-type small switching states with other switching states that do not affect the neutral-  
107 point voltage. Reference [23] demonstrates the ability of the SVPWM method to balance the neutral point  
108 voltage for different regions of the space vector plane, while a new general model was introduced in [24] to  
109 investigate the theoretical and practical limitations of the balancing problems caused by space vector  
110 modulation. A control scheme based on a virtual space vector PWM method is proposed in [25] to control the  
111 neutral-point voltage fluctuation over the full range of the modulation index and load power factor, subject to  
112 the condition that the sum of the three-phase output currents equals zero. The third method reduces voltage  
113 oscillations through a change in circuit topology, as the solution by hardware circuit has its own advantages.  
114 This method incorporates auxiliary components in the traditional NPC three-level inverter circuit and has  
115 proved to be able to achieve good performance to suppress excessive neutral-point voltage fluctuation  
116 effectively at low cost [26].

117 In this paper, two new NPC three-level inverter topologies are proposed. The first is a voltage dependent  
118 NPC three-level inverter (VNPCI), which adopts a voltage compensation method to restrain the neutral point  
119 voltage fluctuation of the DC-link. The second method is a current controlled NPC three-level inverter (CNPCI)  
120 and uses a current compensation method. Both two new inverter topologies are incorporated in a SAPF. The  
121 remainder of this paper is organised as follows. The principle of the SAPF is described in Section 2. The circuit  
122 architectures, their principles of operation and mathematical models describing voltage and current dependent  
123 inverters are outlined in Section 3 and Section 4, respectively. Simulation results of the inverter models and the  
124 performance of the SAPF under typical balanced and unbalanced working load conditions are shown and  
125 discussed in Section 5. Conclusions and suggestions for future work are given in Section 6.

## 127 2. Shunt active power filter (SAPF)

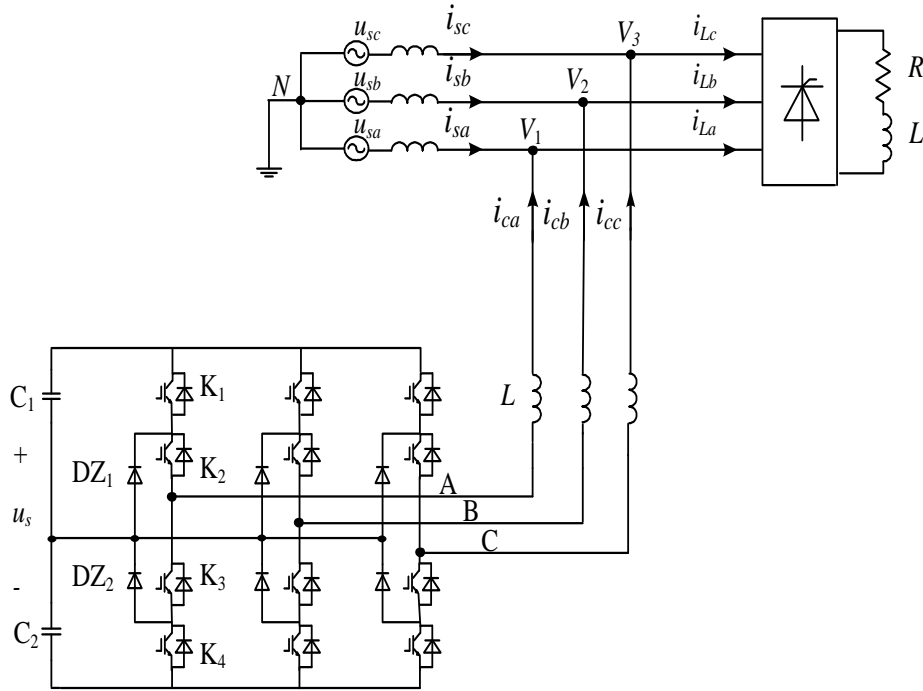


**Figure 2.** A SAPF based on the neutral point clamped (NPC) three-level inverter

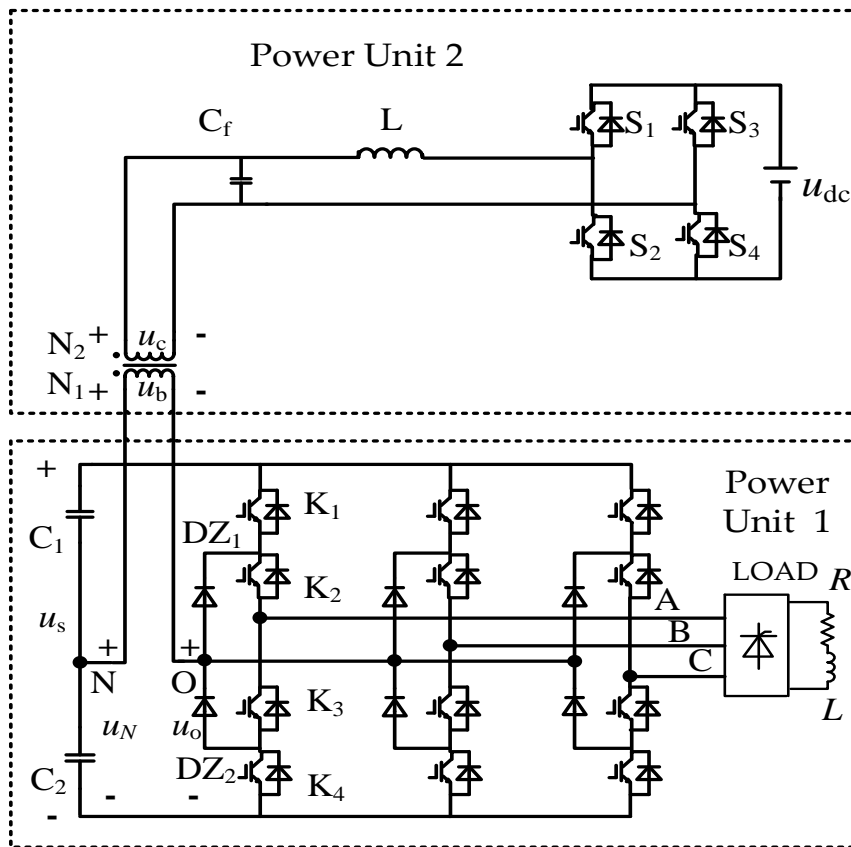
Figure 2 shows a SAPF based on the NPC three-level inverter. In this figure,  $u_{sa}$ ,  $u_{sb}$ ,  $u_{sc}$  are the three-phase alternating-current supplies; the load is nonlinear, generating harmonic currents;  $i_{sa}$ ,  $i_{sb}$ ,  $i_{sc}$  and  $i_{La}$ ,  $i_{Lb}$ ,  $i_{Lc}$  are grid currents and load currents, respectively;  $i_{ca}$ ,  $i_{cb}$ ,  $i_{cc}$  are compensation currents provided by the SAPF, which are used to eliminate harmonic currents in the grid. The SAPF is essentially composed of two major components, namely a conventional NPC three-level inverter and an associated control scheme. In the inverter circuit,  $K_1$ ,  $K_2$ ,  $K_3$ ,  $K_4$  are IGBT (insulated gate bipolar transistor) power switches, while  $DZ_1$ ,  $DZ_2$  are clamp diodes; note that only the components of one inverter arm are labeled for simplicity. The DC bus voltage is split in half using two DC capacitors,  $C_1$  and  $C_2$ , and into three voltage levels,  $u_s$ , 0, and  $-u_s$ , via clamping diodes. The control scheme detects the load currents in real time, which are used to calculate command signals for the IGBT switches. The inverter then works as a signal amplification circuit, producing appropriate compensation currents. This compensation current is equal but opposite to the harmonic currents, which can be overlaid to the load currents, thus eliminating the harmonic currents generated by the nonlinear load.

### 3. Voltage compensated NPC inverter (VNPCI)

#### 3.1. Inverter circuit

The schematic diagram of the VNPCI circuit is shown in Fig. 3. Essentially, the circuit consists of two parts. Power unit 1 is associated with the conventional NPC three-level inverter, as described in the preceding section. In order to reduce excessive neutral-point voltage fluctuations across the DC-link capacitors, this paper considers the application of an active voltage compensation method in which the controllable voltage source is used in series between the neutral point of the DC-link and the neutral point of the three-phase bridge circuit. This voltage source is used in order to compensate for voltage fluctuations across the three-phase bridge arm of the inverter. The voltage at the neutral-point of the three-phase bridge arm is detected in real time and compared with a reference voltage, producing an appropriate value for the compensation voltage. Subsequently, the voltage source generates an equal but opposite voltage, thus reducing the voltage fluctuation across the inverter.

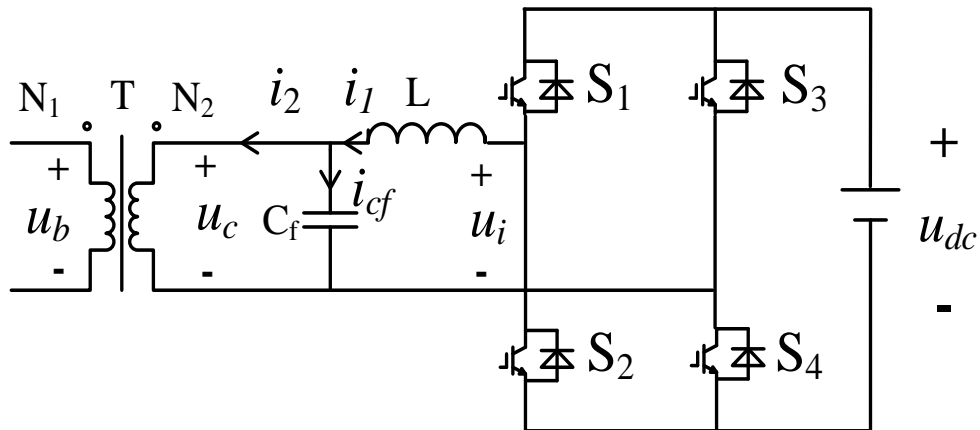
Power unit 2 is an active voltage compensation device, which in essence is a single-phase full-bridge inverter. The device works as a controllable voltage source and is connected in series between the neutral point of the three-phase bridge arm and the neutral point of the DC-link through a coupling transformer. The variables  $u_o$  and  $u_N$  denote the neutral point voltage across the three-phase bridge arm and the DC-link capacitors, respectively;  $u_c$  and  $u_b$  are the voltages across the primary and secondary sides of the transformer, respectively, for which  $u_b$  is used as the compensating voltage;  $u_s$  is the DC-link voltage applied across the capacitors.



162  
163

Figure 3. Schematic diagram of the voltage compensated NPC inverter

164 3.2. The active voltage compensation device



165  
166

Figure 4. Schematic diagram of the active voltage compensation device

167 The voltage compensation device is shown in Fig. 4. It is composed of a single-phase, full-bridge inverter  
168 circuit, where  $S_1, S_2, S_3, S_4$  are IGBT power switches;  $T$  is the coupling transformer with a transformation ratio  
169 of  $n$ ; the inductor  $L$  and the capacitor  $C_f$  form a LC filter that removes unwanted switching harmonics from the  
170 inverter output.

171 Now consider the mathematical model of the voltage compensation device. In the circuit illustrated in Fig.  
172 4,  $u_{dc}$  is a DC voltage applied to the single-phase full-bridge inverter;  $u_i$  is the voltage output of the single-phase  
173 inverter;  $i_1$  is the current through the filter inductor;  $i_2$  is the transformer primary side current;  $i_{cf}$  is the current  
174 passing through the filter capacitor.

175 For an ideal transformer (i.e., no losses and no leakage flux between the primary and secondary windings),

$$u_b = n \left( u_i - L \frac{di_l}{dt} \right) \quad (1)$$

176

177

Hence, for the NPC inverter shown in Fig. 3, the voltage due to the introduction of the compensating voltage  $u_b$  can be obtained via the following equations. In the ideal situation, three-phase bridge arm voltage  $u_o$  should be equal to the half DC-link voltage, i.e.,  $0.5u_s$ .

178

179

$$u_N - u_b = u_o \quad (2)$$

180

$$u_N - n \left( u_i - L \frac{di_l}{dt} \right) = 0.5u_s \quad (3)$$

181

182

For the voltage output of the single-phase inverter  $u_i$

183

$$u_i = S^* u_{dc} \quad (4)$$

184

where  $S^*$  represents the switching function; if  $S_1$  and  $S_4$  are switched on while  $S_2$  and  $S_3$  are switched off, then  $S^*=1$ ; if  $S_1$  and  $S_4$  are switched off while  $S_2$  and  $S_3$  are switched on, then  $S^*=-1$ .

185

186

Substituting (4) into (3) gives

187

$$u_N - n \left( S^* u_{dc} - L \frac{di_l}{dt} \right) = 0.5u_s \quad (5)$$

188

Therefore, the state equations of this active voltage compensation device can be described as,

189

$$\frac{du_c}{dt} = \frac{1}{C_f} (i_1 - i_2) \quad (6)$$

190

$$\frac{di_l}{dt} = \frac{1}{L} (u_i - u_c) \quad (7)$$

191

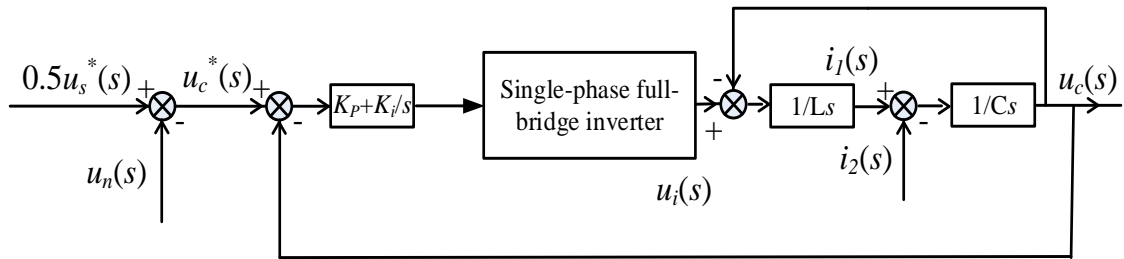
192

The resulting control scheme of the active voltage compensation device is shown in Fig. 5. It illustrates the operating principle of active voltage compensation device as controlled by this scheme. In this diagram, the voltage  $0.5u_s^*(s)$  refers to half of the DC-link voltage under balanced capacitors;  $u_n(s)$  is the DC-link neutral-point voltage measured in real time;  $u_c^*(s)$  is the reference compensating voltage;  $u_i(s)$  is the output voltage of the single phase full bridge inverter circuit;  $u_c(s)$  is the transformer primary side voltage;  $i_l(s)$  is the current in the filter inductor; and  $i_2(s)$  is the transformer primary side current. The compensating voltage  $u_c^*(s)$  is obtained by calculating the difference between the measured neutral-point voltage of DC-link and half of the ideal DC-link voltage. The error voltage between  $u_c^*(s)$  and  $u_c(s)$  is then used for generating PWM signals based on the triangular wave modulation method, which are then used to control the voltage output of the single-phase inverter at a desired level. A PI controller, represented by  $K_p + K_i/s$ , is used because it can provide a compensating voltage output more accurately, thus improving performance further.

199

200

201



202

203

**Figure 5.** The control scheme for the active voltage compensation device

204

#### 4. Current compensated NPC inverter (CNPCI)

205

##### 4.1. Inverter circuit

206

207

As described above, the primary reason causing neutral-point voltage fluctuation across the DC-link is the current that flows in to or out of the neutral points in the circuit. The varying current will lead to charge-discharge phenomena associated with the capacitors through the neutral-points in the circuit, resulting in a fluctuation in the neutral-point voltage. The voltage fluctuation can be alleviated naturally through the use of an active current compensation scheme in which a controllable current source is connected in shunt with one of the DC capacitors. This controllable current source is used to compensate for the current flow between the

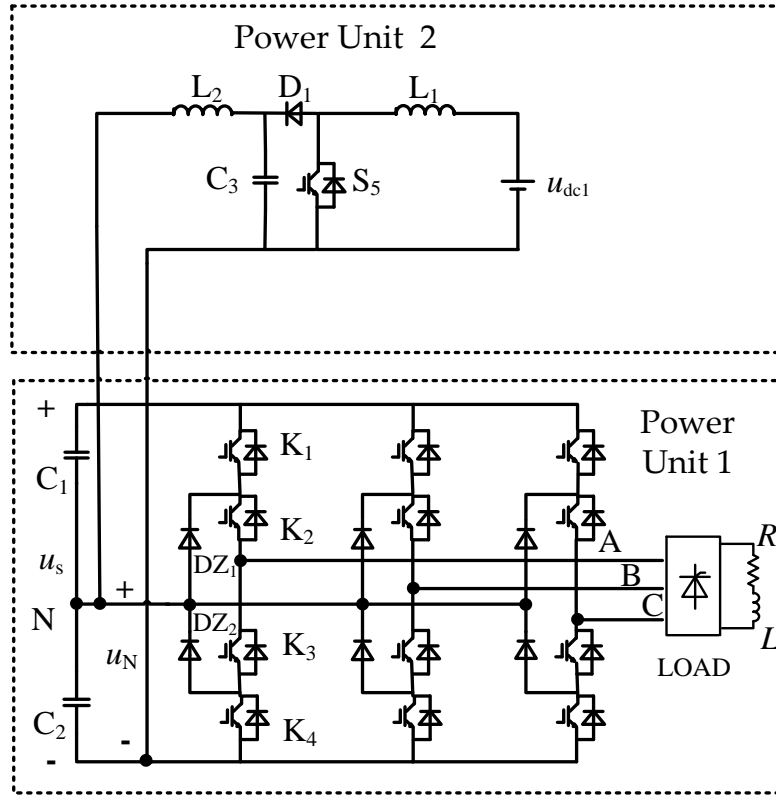
208

209

210

211

212 neutral point of DC-link capacitors and the neutral point of three-phase bridge circuit. It can further suppress  
 213 neutral-point voltage fluctuations because, if this scheme is applied effectively, there is approximately zero  
 214 current flowing between the neutral points in the inverter.  
 215  
 216



217

218

**Figure 6.** Schematic diagram of the current compensation NPC inverter

219

220

221

222

223

224

225

226

227

228

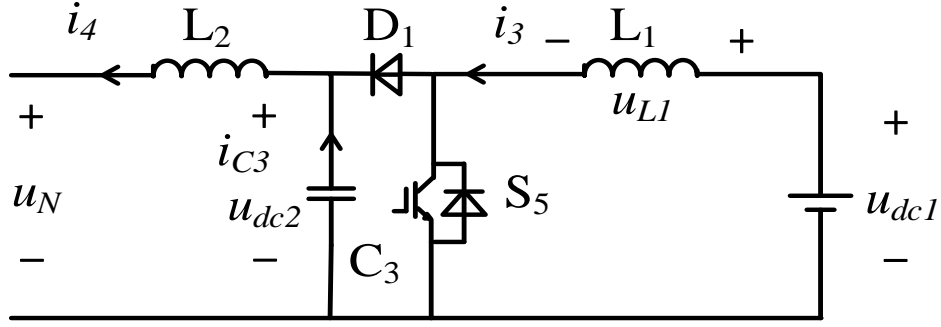
229

The schematic diagram of CNPCI is shown in Fig. 6. It also consists of two parts: part 1 is the conventional NPC three-level inverter and part 2 is the proposed active current compensation device. The compensation device is essentially a boost DC/DC conversion circuit, which works as a current source. The current flowing between the neutral points of the inverter is detected in real time, and an equal but opposite current is then generated through the current compensation device, offsetting the current flow between the neutral points in the inverter. Thus, the charge-discharge phenomenon of DC capacitors through DC-link neutral-point can be restrained effectively. The effectiveness of the current compensation device relies on the voltage difference between the boost circuit and the DC-link, which is applied to the inductor ( $L_2$  in Fig. 6), thus producing a compensation current for the DC capacitor.

230

4.2. Inverter circuit

231



232

233

**Figure 7.** Schematic diagram of the active current compensation device

234

235

236

237

238

239

240

241

242

Fig. 7 shows the proposed active current compensation device, essentially a boost DC/DC converter circuit, where  $S_5$  is the IGBT power switch;  $D_1$  is a diode preventing reverse current flow;  $L_1$  is a power inductor used for energy storage;  $L_2$  and  $C_3$  form a LC filter for the circuit. Now consider the mathematical model of the active current compensation device. In the circuit,  $u_{dc1}$  is the voltage input of the boost DC/DC converter;  $u_{dc2}$  is the voltage output of the boost DC/DC converter;  $u_N$  is the DC-link neutral-point voltage;  $i_{c3}$  is the current in the capacitor  $C_3$ ;  $i_3$  is the current in the inductor  $L_1$ ;  $i_4$  is the compensating current. Suppose  $i_{c3(off)}$  and  $i_{c3(on)}$  are the current in capacitor  $C_3$  when the switching device  $S_5$  is off and on, respectively;  $u_{L1(off)}$  is the voltage across the inductor  $L_1$  when the switching device  $S_5$  is off while  $u_{L1(on)}$  is the voltage across the inductor  $L_1$  when the switch  $S_5$  is on.

243

244

When the switching device  $S_5$  is turned on, the state equations of the current compensation device can be described as,

245

$$\begin{cases} L_1 \frac{di_3}{dt} = u_{dc1} = u_{L_1(on)} \\ C_3 \frac{du_{dc2}}{dt} = i_4 = i_{C_3(on)} \end{cases} \quad (8)$$

246

When the switching device  $S_5$  is turned off, the above equation can be written as

247

$$\begin{cases} L_1 \frac{di_3}{dt} = u_{dc1} - u_{dc2} = u_{L_1(off)} \\ C_3 \frac{du_{dc2}}{dt} = i_4 - i_3 = i_{C_3(off)} \end{cases} \quad (9)$$

248

During one switching cycle,  $T_s$ , the average voltage across the inductor  $L_1$  is,

249

$$\bar{u}_{L_1} = \frac{1}{T_s} \left[ \int_t^{t+DT_s} u_{L_1(on)}(\tau) d\tau + \int_{t+DT_s}^{t+T_s} u_{L_1(off)}(\tau) d\tau \right] \quad (10)$$

250

$$\bar{u}_{L_1} = D u_{dc1} + (1 - D)(u_{dc1} - u_{dc2}) \quad (11)$$

251

252

where  $D$  represents the duty cycle of the switching device  $S_5$ , i.e., the proportion of time during which  $S_5$  is operated.

253

During one switching cycle, the average current in the capacitor  $C_3$  is equal to

254

$$\bar{i}_{C_3} = \frac{1}{T_s} \left[ \int_t^{t+DT_s} i_{C_3(on)}(\tau) d\tau + \int_{t+DT_s}^{t+T_s} i_{C_3(off)}(\tau) d\tau \right] \quad (12)$$

255

$$\bar{i}_{C_3} = D i_4 + (1 - D)(i_4 - i_3) \quad (13)$$

256

257

258

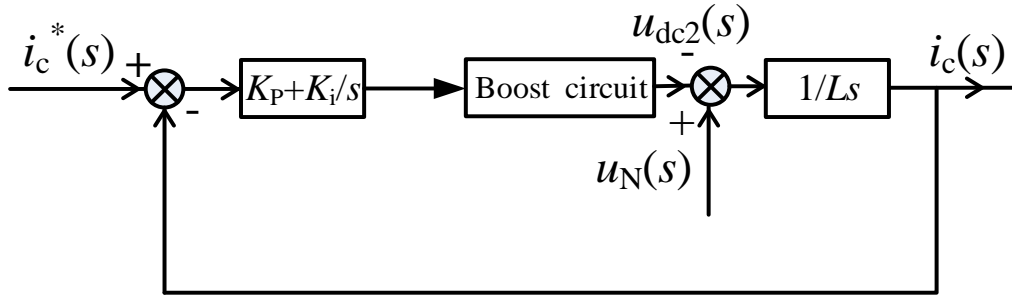
It is well known that the average voltage across an inductor and the average current in a capacitor should be zero during a switching cycle. Hence, under steady state, the current compensation device can be described as follows



$$\begin{cases} u_{dc2} = \frac{1}{1-D} u_{dc1} \\ i_4 = (1-D) i_3 \end{cases} \quad (14)$$

259  
260  
261  
262  
263  
264  
265  
266  
267

A control scheme, designed for the active current compensation device, can be derived from this model, as shown in Fig. 8. In this circuit,  $u_{dc2}(s)$  is the voltage output of the boost DC/DC converter;  $u_N(s)$  is the DC-link neutral-point voltage measured in real time. The reference compensating current  $i_c^*(s)$  is obtained by the real-time detection of the current flowing between the neutral points of the inverter. The current  $i_c(s)$  is the compensation current generated by the boost circuit. The error current between  $i_c^*(s)$  and  $i_c(s)$  is then used to generate PWM signals. This signal is based on the triangular wave modulation method, producing a compensating current at the desired level. As with the voltage compensation scheme, a PI controller, represented by  $K_p+K_i/s$ , is used because it generates a more accurate compensation current.



268

**Figure 8.** The control scheme for the active current compensation device

269

## 270 5. Results and analysis

### 271 5.1. The inverters

272 Models of the voltage compensation device and the current compensation device have been built using  
273 Simulink SimPowerSystems, as described above and shown in Fig. 3 and Fig. 6, respectively. The parameters  
274 used in the models are given in Table 1. The DC-link voltage is 3 kV, a level commonly used in medium voltage  
275 power drives; the switching frequency for the NPC three-level inverter is 1 kHz; and the switching frequencies  
276 used to control the single-phase inverter for the voltage- and current-compensation device are both set to 10  
277 kHz. In order to evaluate the dynamic performance of the proposed inverters, a nonlinear load is used in this  
278 study. This load consists of a three-phase rectifier with a resistive (4Ω) and inductive (15mH) load. The use of  
279 a nonlinear load increases the neutral-point voltage fluctuation of the DC-link, because the nonlinear load draws  
280 a current that is not necessarily sinusoidal, hence generating harmonic currents. The NPC three-level inverter  
281 is used with a constant voltage output control strategy, based upon space voltage vector modulation (SVPWM).  
282 The error voltage between the NPC three-level inverter output voltage and the reference voltage is processed  
283 by a PI controller, which is then used as the input signal for SVPWM to generate appropriate PWM signals. This  
284 control scheme has a higher efficiency for controlling the DC-side voltage than the equivalent sine pulse width  
285 modulation method.

286

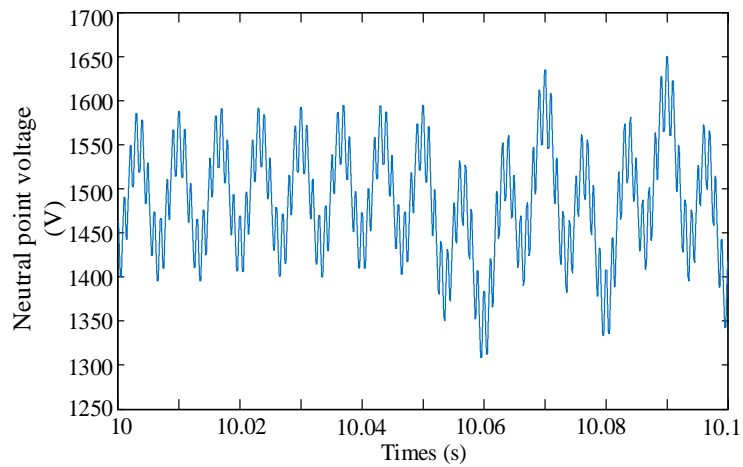
Table 1. Parameters used in the VNPCI and CNPCI inverters

| Parameters of the VNPCI                    |             | Parameters of the CNPCI |             |
|--|-------------|-------------------------|-------------|
| Parameters                                 | Value       | Parameters              | Value       |
| $u_{dc}$                                   | 500 V       | $u_{dc1}$               | 100 V       |
| $C_f$                                      | 50 $\mu$ F  | $L_1$                   | 10 mH       |
| $L$  | 0.4 mH      | $L_2$                   | 0.5 mH      |
|  |             | $C_3$                   | 800 $\mu$ F |
| Parameters of the NPC three-level inverter |             |                         |             |
| $u_s$                                      | 3000 V      |                         |             |
| $C_1, C_2$                                 | 500 $\mu$ F |                         |             |

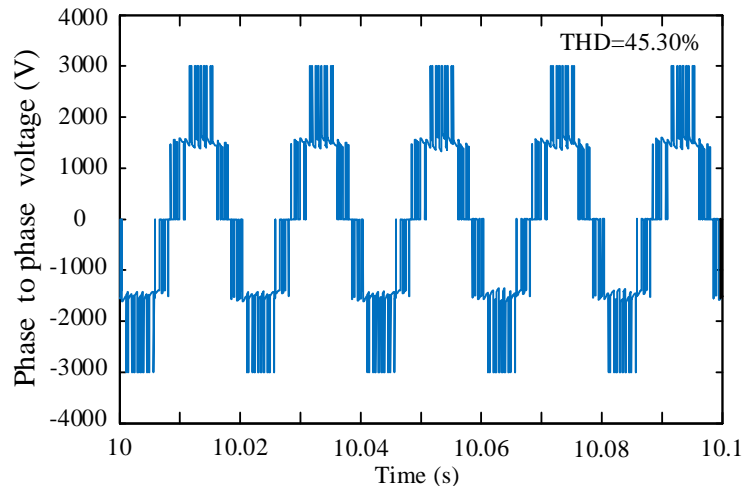
287  
288  
289  
290  
291  
292  
293  
294  
295  
296  
297  
298  
299  
300  
301

In real world applications, the load can be either in a balanced or unbalanced condition. An unbalanced load added to the three phase output voltage of an inverter can result in greater fluctuations in the neutral-point voltage across the DC-link. In the simulation, the inverters are initially connected to a balanced nonlinear load, and resistive ( $8\Omega$ ) and inductive ( $1.5\text{mH}$ ) loads are then applied between phase A and phase B in order to evaluate the dynamic performance of the proposed compensation devices under a unbalanced load condition. The unbalanced load occurs at  $10.05\text{ s}$  and lasts for  $0.05\text{ s}$ .

Firstly, a conventional NPC three-level inverter, under balanced and unbalanced working load conditions, has been modelled and investigated. Fig. 9(a) and (b) show the waveform of the neutral-point voltage  $u_o$ , the phase A to phase B voltage  $u_{AB}$  of the conventional inverter. The neutral-point voltage fluctuation across the DC-link is severe, even in the balanced load condition; the range of the fluctuation reaches a value of  $200\text{V}$ . During the unbalanced load condition, applied from  $10.05\text{s}$  to  $10.1\text{s}$ , it can be seen the neutral-point voltage fluctuation range increases to  $300\text{V}$ . The THD (total harmonic distortion) of the output voltage waveform across the inverter is  $45.30\%$ .



a. Voltage waveform of neutral-point voltage  $u_o$



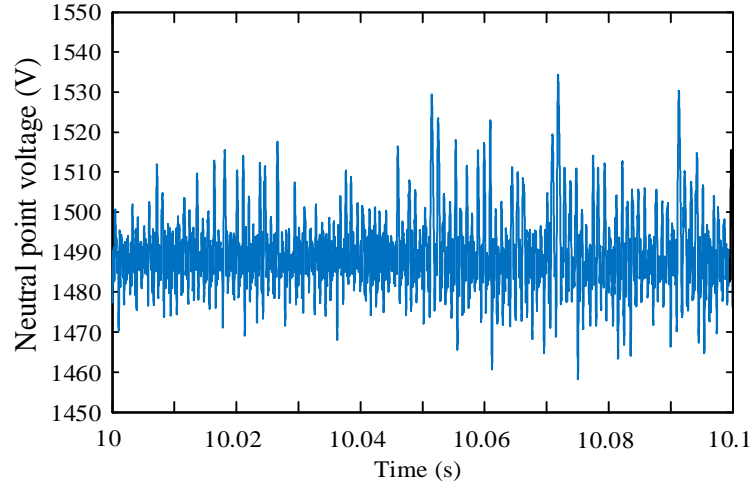
b. Voltage waveform of phase A to phase B voltage  $u_{AB}$

302  
303  
304

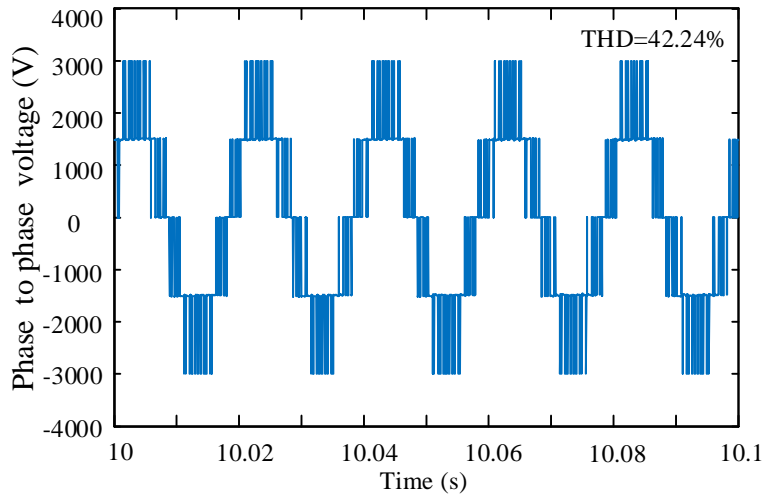
305  
306  
307

**Figure 9. Voltage waveforms of the conventional NPC in a load swell**

308 Fig. 10(a) and (b) show the waveform of the neutral-point voltage  $u_o$ , the phase A to phase B voltage  $u_{AB}$   
309 of the proposed voltage compensated NPC inverter under the balanced and unbalanced working load conditions.  
310 With the voltage compensation device being added, the neutral-point voltage fluctuation of DC-link is  
311 suppressed effectively, being reduced to  $40\text{V}$ . Similarly, an unbalanced load is applied at  $10.05\text{ s}$ , lasting  $0.05$   
312 s. The neutral-point voltage fluctuation of DC-link is reduced to  $75\text{V}$  under the unbalanced load condition. The  
313 THD of output voltage of the inverter is  $42.24\%$ .



a. Voltage waveform of neutral-point voltage  $u_o$

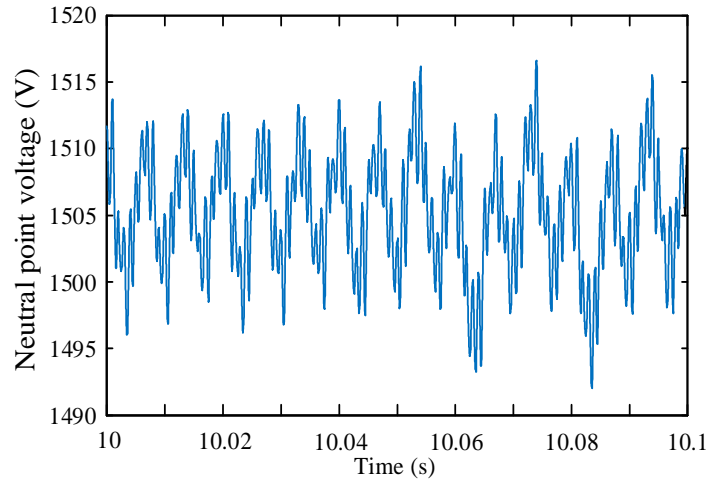


b. Voltage waveform of the phase A to phase B voltage  $u_{AB}$

**Figure 10. Voltage waveforms of the proposed VNPCI in a load swell**

Fig. 11(a) and (b) shows the neutral-point voltage  $u_o$ , the phase A to phase B voltage  $u_{AB}$  of the proposed current compensated NPC inverter under the balanced and unbalanced working load conditions. With the current compensation device being added, the neutral-point voltage fluctuation of DC-link is suppressed further to 18V. Under the unbalanced load condition between 10.05 s and 10.1 s, the neutral-point voltage fluctuation of DC-link is reduced to 25V. The THD of output voltage of the NPC three-level inverter is 42.08%.

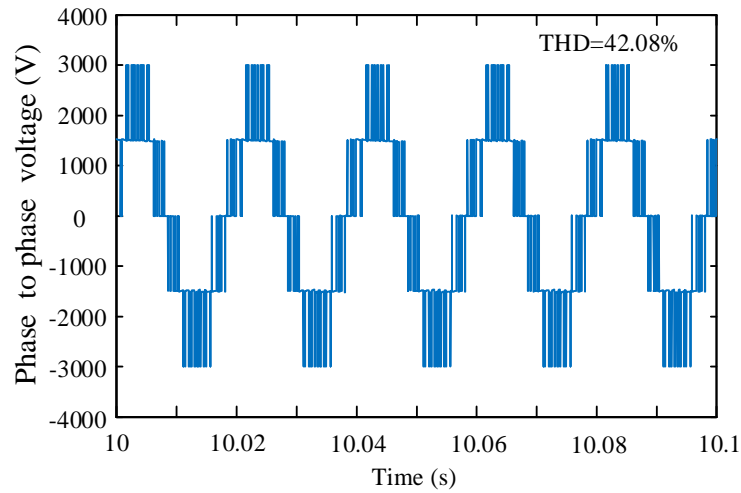
The results clearly show that the current compensated NPC inverter (CNPCI) has a better performance than the voltage compensated NPC inverter (VNPCI). Fig. 10 and Fig. 11 demonstrate that the CNPCI can restrict the neutral-point voltage fluctuation of the DC-link to 0.6% and 0.83%, respectively, when the CNPCI works under typical balanced and unbalanced working load conditions. However, the VNPCI restrains the neutral-point voltage fluctuation of DC-link to 1.2% and 2.3%, respectively, in the same conditions. The waveform comparison of neutral-point voltage  $u_o$  produced in different condition is shown in Fig. 12. The effect of the switching frequency on the output performance was also investigated. It was found a frequency higher than 2 kHz can produce acceptable results but the use of 10 kHz switching frequency produced the best results although it might be too fast for the device to work at such a high voltage level.



335

336

a. Voltage waveform of neutral-point voltage  $u_o$



337

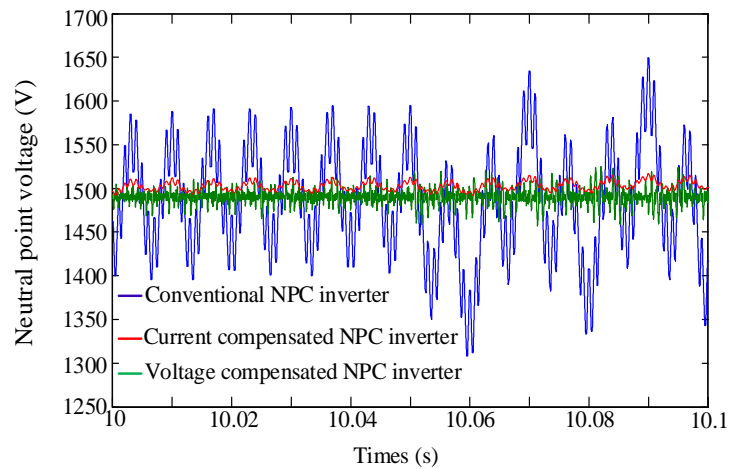
338

b. Voltage waveform of the phase A to phase B voltage  $u_{AB}$

**Figure 11.** Voltage waveforms of the proposed CNPCI in a load swell

339

340



341

342

**Figure 12.** Waveform comparison of the neutral-point voltage  $u_o$  produced in the three inverter topologies

343

344

345

346

347

The VNPCI only eliminates the voltage fluctuation at the neutral-point of three-phase bridge arm; there is still fluctuation of the neutral-point voltage of the DC-link. This means the fluctuation problem cannot be eliminated thoroughly. However, the CNPCI can eliminate the neutral-point voltage fluctuation of the DC-link more effectively because the CNPCI offsets the current that flows between the neutral point of the DC-link

348 capacitors and the neutral point of the three-phase bridge circuit in the inverter, which is the cause of the voltage  
349 fluctuation. In addition, for the VNPCI, an isolated transformer is required, which should be able to handle  
350 several harmonic components without entering to the saturation region in the primary side and handle secondary  
351 side voltage range quickly to compensate the zero sequence voltage generated at the NPC converter. A  
352 complicated control scheme is therefore needed to overcome these problems [27]. On the contrary, the CNPCI  
353 avoids using the isolated transformer; the cost to manufacture and assemble the CNPCI is therefore lower than  
354 the VNPCI; the CNPCI requires only one IGBT power switching device (the most expensive component in the  
355 circuit), while the VNPCI needs four IGBT power switches and a coupling transformer. Thus, the CNPCI offers  
356 a more cost-effective performance.

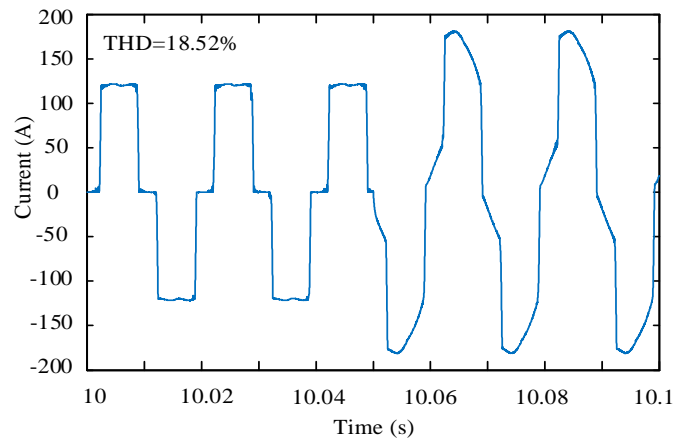
357 The selection of PI control parameters were made by trial and error, aiming to achieve an optimal  
358 performance from tests. The proportional response can be adjusted by multiplying the error (i.e., the voltage  
359 difference in the case of the VNPCI and the current difference in the case of the CNPCI) by the proportional  
360 gain  $K_p$ . The integral term in the PI controller is the sum of the instantaneous error over time, thus giving the  
361 accumulated offset, which is then multiplied by the integral gain  $K_i$ . For the VNPCI, the selected value of  $K_p$   
362 and  $K_i$  are 5 and 10, respectively, while, for the CNPCI, the selected value of  $K_p$  and  $K_i$  are 10 and 0.5,  
363 respectively. Results have shown that the use of these parameters can provide an improved performance of the  
364 controllers.

## 365 5.2. The shunt active power filters (SAPF)

366 The two proposed inverters are now applied in the SAPF that is indispensable part of the grid system. The  
367 SAPFs incorporating with the current compensated NPC inverter and the voltage compensated NPC inverter  
368 have been built and simulated. One of the typical SAPF applications is in the AC 400V DG system [28]; but  
369 unlike the normal inverter, in order to satisfy the working condition in three phase power system, the DC link  
370 voltage of SAPF must be over 3 times higher than the phase voltage. Thus, the NPC three-level inverter is very  
371 suitable to apply in SAPF due to high DC link voltage. The parameters used in the model are defined as follows:  
372 DC link voltage of SAPF is 800V; supply fundamental frequency  $f = 50\text{Hz}$ ; filter line inductance  $L_s = 2\text{mH}$ ;  
373 other parameters used for the inverters are referred to Table 1. It is noteworthy that the use of a low DC link  
374 voltage, rather than the 3000V previously discussed, was to assess the performance of the proposed inverters  
375 for this particular application in SAPF. As mentioned above, nonlinear loads are often connected in the power  
376 grid and the load condition will affect the work efficiency of the NPC three-level SAPF. The SAPF is firstly  
377 connected to a balanced nonlinear load and then to an unbalanced load emulated by a resistive ( $8\Omega$ ) and  
378 inductive ( $1.5\text{mH}$ ) load being applied between phase A and phase B. The unbalanced load also occurs at 10.05  
379 s and lasts 0.05 s.

380 Firstly, a SAPF based on the traditional NPC three-level inverter connected with the three phase nonlinear  
381 load, as shown in Fig. 2, has been investigated under the balanced and unbalanced working load conditions.  
382 Fig. 13 show the waveform of grid current of phase A, as an example. The grid current distorts heavily in both  
383 balanced and unbalanced load condition, and the THD of the grid current is 18.52%.

384



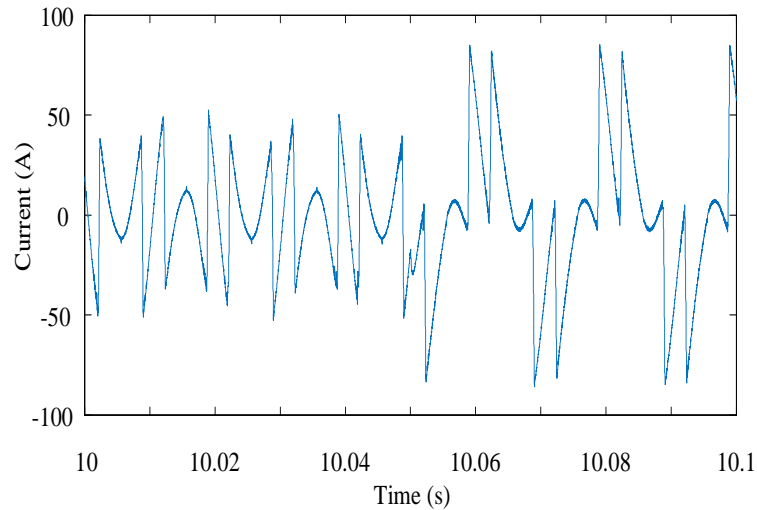
385

386

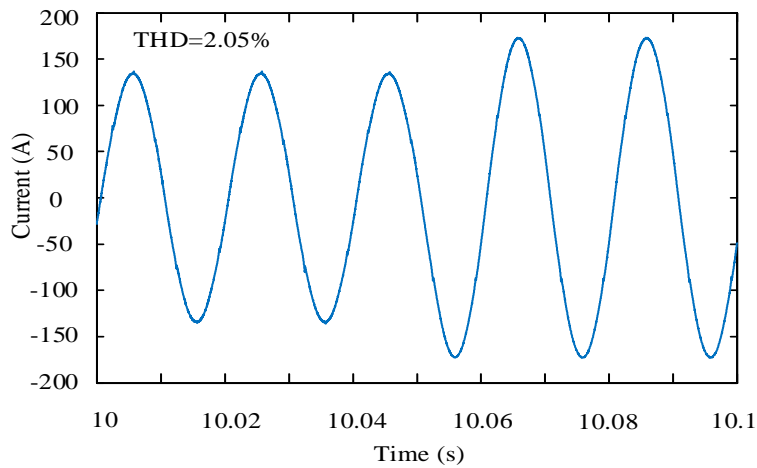
**Figure 13.** Waveform of phase-A current of the power grid under the nonlinear load

387  
388  
389  
390  
391  
392  
393  
394  
395  
396

Fig. 14 shows the waveform of the filter output of phase A, i.e., the currents  $i_{ca}$ ,  $i_{cb}$  and  $i_{cc}$  as shown in Fig. 2, and the grid currents of the proposed VNPCI three-level SAPF, i.e., the currents  $i_{sa}$ ,  $i_{sb}$  and  $i_{sc}$  as shown in Fig. 2, under the typical balanced and unbalanced working load conditions. Essentially, the filter output currents are effective to compensate the harmonics being injected from nonlinear loads, hence improving the quality of the grid currents. The frequency component is dominant at 50 Hz while other harmonic components in phase-A current are now eliminated effectively. The THD of the grid current is reduced to 2.05%. Fig. 15 shows the waveform of the grid currents of the proposed CNPCI three-level SAPF under typical balanced and unbalanced working load conditions. It can be seen that the harmonic currents in phase A can be eliminated more effectively. The THD of the grid current is reduced further to 1.7%.



a. Waveform of the phase-A current in the filter output



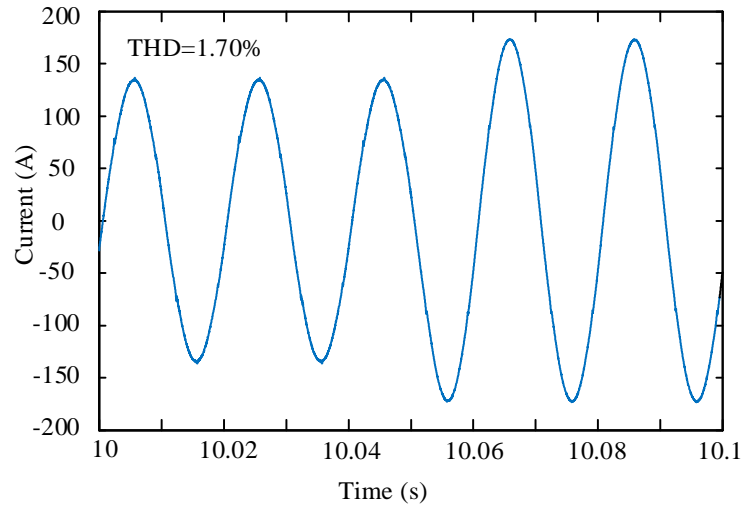
b. Waveform of the phase-A current in the power grid

397  
398  
399

400  
401

402  
403

**Figure 14.** Waveform of the phase-A currents in the filter output and the power grid employing the proposed VNPCI three-level SAPF



404

405

**Figure 15.** Waveform of the power grid currents employing the proposed CNPCI three-level SAPF

406

## 6. Conclusions

407

408

409

410

411

412

413

414

415

416

417

418

419

420

421

422

423

424

The paper presents two new NPC three-level inverter topologies in order to eliminate excessive voltage fluctuation happened at the neutral-point of DC-link capacitors of the inverter. The first is voltage dependent, which adopts a voltage compensation method to restrain the neutral point voltage fluctuation. The second is current dependent, using a current compensation method to restrict the voltage fluctuation. The results show that both topologies can suppress the neutral-point voltage fluctuation of the DC-link effectively under typical balanced and unbalanced working load conditions. The current compensated NPC inverter outperforms the voltage compensated NPC inverter. Furthermore, these compensated NPC three-level inverters are applied to a shunt active power filter in the grid lines. It is shown that the proposed approaches are effective and feasible for eliminating harmonic currents and therefore improving power quality of the grid system when connected with nonlinear loads.

Future work will focus on experimental testing of the proposed NPC three-level SAPFs to further verify their performance. Optimal selection of PI control parameters for the inverters will also be investigated in order to further optimize system performance under different load conditions. In addition, the application of the proposed current compensated NPC inverter is being considered in both a wind power generation system and a small grid system in the laboratory in order to address the power quality issues related to inverter-coupled generation and associated loads.

## 425 References

- 426 1. Pepermans G, Driesen J, Haeseldonckx D, Belmans R, D'haeseleer W. Distributed generation: definition,  
427 benefits and issues, *Energy Policy* 2005; 33: 787-798.
- 428 2. Pouresmaeil E, Montesinos-Miracle D, Gomis-Bellmunt O, Sudrià-Andreu A. Instantaneous active and  
429 reactive current control technique of shunt active power filter based on the three-level NPC inverter,  
430 *International Transactions on Electrical Energy Systems* 2011; 21: 2007-2022.
- 431 3. Allmeling J H. A control structure for fast harmonics compensation in active filters, *IEEE Transactions on*  
432 *Power Electronics* 2004; 19(2): 508-514.
- 433 4. Liang W, Donglai Z, Yi W, Bin W, Hussain S A. Power and voltage balance control of a novel three-phase  
434 solid-state transformer using multilevel cascaded H-bridge inverters for microgrid applications, *IEEE*  
435 *Transactions on Power Electronics* 2016; 31(4): 3289-3301.
- 436 5. Roodsari B N, Nowicki E P. Fast space vector modulation algorithm for multilevel inverters and its  
437 extension for operation of the cascaded H-bridge inverter with non-constant DC sources, *IET Power*  
438 *Electronics* 2013; 6: 1288-1298.
- 439 6. Ke M, Frede B. The impact of power switching devices on the thermal performance of a 10 MW wind  
440 power NPC converter, *Energies*, 2012; 5(7): 2559-2577.
- 441 7. Muyeen S M, Takahashi R, Tamura J. Wind power and hydrogen generation system with cooperatively  
442 controlled three-level NPC-VSC based energy capacitor, *International Transactions on Electrical Energy*  
443 *Systems* 2010; 20: 1071-1081.
- 444 8. Zaveri T, Bhalja B R, Zaveri N. Load compensation using DSTATCOM in three-phase, three-wire  
445 distribution system under various source voltage and delta connected load conditions, *International Journal*  
446 *of Electrical Power & Energy System*, 2012; 41: 34-43.
- 447 9. Saad S, Zellouma L. Fuzzy logic controller for three-level shunt active filter compensating harmonics and  
448 reactive power, *Electric Power Systems Research* 2009; 79: 1337-1341.
- 449 10. Celanovic N, Boroyevich D. A comprehensive study of neutral-point voltage balancing problem in three-  
450 level neutral-point-clamped voltage source PWM inverters, *IEEE Transactions on Power Electronics* 2000;  
451 15: 242-249.
- 452 11. Ui-Min C., Frede B, Kyo-Beum L. Method to Minimize the Low-Frequency Neutral-Point Voltage  
453 Oscillations With Time-Offset Injection for Neutral-Point-Clamped Inverters, *IEEE Transactions on*  
454 *Industry Applications*, 2015; 51: 1678-1691.
- 455 12. Rodriguez J, Bernet S. A Survey on Neutral-Point-Clamped Inverters, *IEEE Transactions on Industrial*  
456 *Electronics* 2010; 57: 2219-2230.
- 457 13. Helle L, Nielsen S M, Enjeti P. Generalized discontinuous DC-link balancing modulation strategy for three-  
458 level inverters *Power Conversion Conference, Osaka, Japan, 2002*; 2: 359-366.
- 459 14. Yazdani A, Iravani R. Generalized state-space averaged model of the three-level NPC converter for  
460 systematic DC-voltage-balancer and current-controller design, *IEEE Transactions on Power Delivery*, 2005;  
461 20: 1105-1114.
- 462 15. Zaragoza J, Pou J, Ceballos S, Robles E, Jaen C. Voltage-balance compensator for a carrier-based  
463 modulation in the neutral-point-clamped converter, *IEEE Transactions on Industrial Electronics*, 2009; 56:  
464 305-314.
- 465 16. Ui-Min C, June-Seok L, Kyo-Beum L. New Modulation Strategy to Balance the Neutral-Point Voltage for  
466 Three-Level Neutral-Clamped Inverter Systems, *IEEE Transactions on Energy Conversion* 2014; 29: 91-  
467 100.
- 468 17. Pulikanti S R, Dahidah S A. Voltage balancing control of three-level active NPC converter using SHE-  
469 PWM, *IEEE Transactions on Power Delivery* 2011; 26: 258-267.
- 470 18. Ghennam T, Berkouk E M, Francois B. A novel space-vector current control based on circular hysteresis  
471 areas of a three-phase neutral point- clamped inverter, *IEEE Transactions on Industrial Electronics* 2010;  
472 57: 2669-2678.
- 473 19. Lewicki A, Krzeminski Z, Abu-Rub H. Space-vector pulse width modulation for three-level NPC converter  
474 with the neutral point voltage control, *IEEE Transactions on Industrial Electronics* 2011; 58: 5076-5086.
- 475 20. Xiyu C, Kazerani M. Space vector modulation control of an ac-dc-ac converter with a front-end diode  
476 rectifier and reduced dc-link capacitor, *IEEE Transactions on Power Electronics* 2006; 21: 1470-1478.
- 477 21. Huibin Z, Finney S J, Massoud A, Williams B W. An SVM algorithm to balance the capacitor voltages of  
478 the three-level NPC active power filter, *IEEE Transactions on Power Electronics* 2008; 23: 2694-2702.
- 479 22. Bouhali O, Francois B, Berkouk E M. DC link capacitor voltage balancing in a three-phase diode clamped  
480 inverter controlled by a direct space vector of line-to-line voltages, *IEEE Transactions on Power Electronics*  
481 2007; 22: 1636-1648.
- 482 23. Dongsheng Z, Didier G. R. Experimental comparisons of space vector neutral point balancing strategies  
483 for three-level topology, *IEEE Transactions on Power Electronics* 2001; 16: 872-879.



- 484 24. Nikola C, Dushan B. A comprehensive study of neutral-point voltage balancing problem in three-level  
485 neutral-point-clamped voltage source PWM inverters, IEEE Transactions on Power Electronics 2000; 15:  
486 242-249.
- 487 25. Sergio B, Josep B, Dushan B, Sergio S. The nearest three virtual space vector PWM—A modulation for  
488 the comprehensive neutral-point balancing in the three-level NPC inverter, IEEE Power Electronics Letters  
489 2004; 2: 11-15.
- 490 26. Mishra M K, Joshi A, Ghosh A. Control schemes for equalization of capacitor voltages in neutral clamped  
491 shunt compensator, IEEE Transactions on Power Delivery 2003; 18: 538-544.
- 492 27. Yong L, Yanjian P, Fang L, Denis S, Daniil P, Chonggan L, Long L, Yijia C. A controllably inductive  
493 filtering method with transformer-integrated linear reactor for power quality improvement of shipboard  
494 power system, IEEE Transactions on Power Delivery, 2016.
- 495 28. Shengwei L, Yongli L, Jingliao S, Qiang J, Xuguang L. A novel control algorithm for inverter-based  
496 distributed generation in unbalanced three phase power systems, International Conference on Sustainable  
497 Power Generation and Supply, Nanjing, China, 2009; 1-6.